

Simulation of the Electrical Properties of Conductive ITO Thin Films by Finite Element Analysis

Ning Xia, Youngho Jin and Rosario A. Gerhardt*

School of Materials Science and Engineering, Georgia Institute of Technology, Atlanta, GA USA

Introduction

Finite element analysis (FEA) can be used to study the electrical properties of conductive ITO thin films and assist with determining a more accurate interpretation of the experimental measurements. In our group, previous simulation studies have been conducted for insulating thin films on conductive substrates [1,2]. It was found that changes of electrode size and film thicknesses can cause huge differences in the measured electrical properties and various degrees of measurement error. Most studies of the electrical properties for ITO films have been based on experimental data and very few electrical simulations have been reported [3]. ITO films are usually deposited on insulating substrates. Thus the electrical behavior is completely different from the situations of insulating films on conducting substrates. In this study, ITO films with different measurement configurations and film thicknesses were investigated by FEA using 3D models.

Model Setup and Equations

The FEA tool used in this study was COMSOL Multiphysics 5.3. The simulations here utilized a bi-conjugate gradient stabilized iterative solver in the ac/dc module in the frequency domain in order to implement a finite element method to solve the partial differential equations. The goal is to solve the Maxwell's Equation 1 in terms of the electric potential (V) [4].

$$-\nabla \cdot \left((\sigma + \varepsilon_r \varepsilon_0 \frac{\partial}{\partial t}) \nabla V \right) = 0 \quad (1)$$

where σ is the electrical conductivity of the material, ε_r is the relative permittivity of the material and ε_0 is the vacuum permittivity (8.854×10^{-12} F/m). The problem is then reduced to solving the electric potential in each finite element domain. An AC voltage signal was added to the terminal electrode and the ground electrode was set to a zero potential as a 2-probe method. The current flowing from the terminal to the ground electrode was then extracted. The admittance (Y) can be derived between the terminal electrode and ground electrode using the functions in COMSOL software. Other

dielectric properties such as impedance (Z) and capacitance (C) can also be obtained using Equations 2 and 3:

$$Z^* = \frac{1}{Y^*} = Z' + jZ'' \quad (2)$$

$$C^* = C' + jC'' = \frac{Y''}{\omega} + j \frac{Y'}{\omega} \quad (3)$$

In this simulation study, the ITO films are treated as homogeneous layers without any defects and porosity. The procedure for the modeling setup in FEA is: (1) Choosing the right 3D model and the ac/dc electric currents interface in the COMSOL model wizard; (2) Drawing the film model with or without environment; (3) Building the appropriate mesh; (4) Defining the electrical parameters for each material and boundary; (5) Computing the model by the right solver in the frequency domain study; (6) Converting the calculated data into other electrical properties [5].

Experimental Results

Effects of different measurement configurations for ITO films

Different measurement configurations can be used to measure the impedance of samples. Simulation of different measurement configurations can help predict the impedance measurement results. Parallel-plate and in-plane measurement are two common configurations for impedance tests. In a parallel-plate measurement simulation, the ITO film is deposited onto a conducting substrate. Here we use tungsten carbide (WC) substrates as an example. Another conducting substrate is put on top of the ITO film to form a sandwich structure as shown in Figure 1. Two square WC plates have the same size of 12.7 mm \times 12.7 mm and thickness of 1 mm (which is a common value for substrate thickness). The ITO film is also 12.7 mm \times 12.7 mm but the thickness is 10 μ m. The top WC plate serves as the terminal electrode and the bottom WC plate is the ground electrode. The electrical response of the system can be simulated.

In-plane measurement is another configuration that can be used for obtaining ITO film impedance. A probe station (using WC probes)

is required to work as electrodes on top (Figure 2). In the actual simulation, the thickness of the electrode was ignored to reduce the number of mesh elements. No contact resistances were added between the electrodes and the ITO film to simplify the simulation.

In the simulation model, a 10 μm ITO film is put on top of the substrate (12.7 mm \times 12.7 mm \times 1 mm) and is surrounded by air (15 mm \times 15 mm \times 2 mm) which best represents the real environment. Conducting substrates or insulating substrates may be used for ITO films. For the conducting substrate we used a WC plate, and for the insulating substrate we used quartz glass. Figure 3 shows the comparison of the electric potential maps for ITO films on the two different substrates.

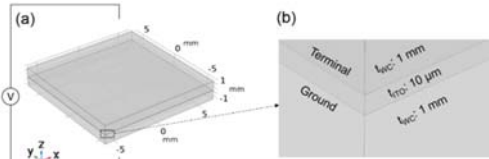


Figure 1. (a) 3D model geometry for the parallel-plate measurement configuration; (b) magnified figure to show the detailed sandwich structure. (12.7 mm \times 12.7 mm \times 1 mm WC plates, 12.7 mm \times 12.7 mm \times 10 μm ITO film)

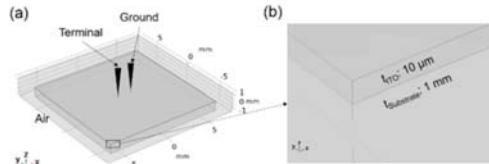


Figure 2. (a) 3D model geometry for the in-plane measurement configuration; (b) magnified figure to show the ITO film on the substrate. (15 mm \times 15 mm \times 2 mm air, 12.7 mm \times 12.7 mm \times 10 μm ITO film, 12.7 mm \times 12.7 mm \times 1 mm substrate, $D = 80 \mu\text{m}$ circular electrodes with a center spacing of 1.5875 mm)

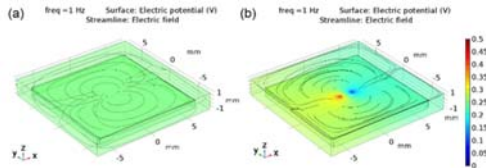


Figure 3. Simulated 3D electric potential map and electric field lines at 1 Hz for (a) ITO film on a conducting substrate; (b) ITO film on an insulating substrate. (15 mm \times 15 mm \times 2 mm air, 12.7 mm \times 12.7 mm \times 10 μm ITO film, 12.7 mm \times 12.7 mm \times 1 mm substrate, $D = 80 \mu\text{m}$ circular electrodes with a center spacing of 1.5875 mm)

On the conducting substrate, the electric potential of the ITO film surface is very low except for the region near the electrodes area.

Conversely, the electric potential for the insulating substrate shows much bigger variance near the electrodes region. The conducting mechanism is different for these two cases. This can be easily noticed in the 2D current density maps shown in Figure 4. When measuring an ITO film on a conducting substrate, only the ITO region under electrodes has a high current density. The current passes through the ITO film and the WC substrate has a major contribution to the current path (Figure 4(a, c)). As a comparison, the main current path for an ITO film on an insulating substrate remains in the ITO film between two electrodes (Figure 4(b, d)). The current density spreads out from the electrodes and flows in the plane parallel to the substrate. Thus the current density is very low in the glass substrate.

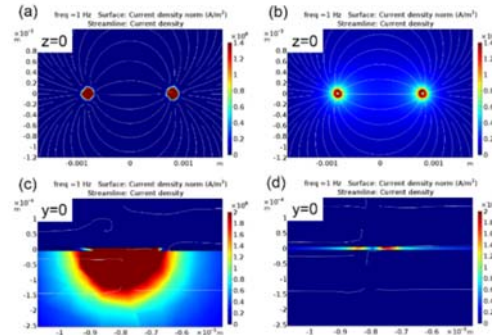


Figure 4. 2D simulated surface current density map at $z=0$ for ITO film (a) on a conducting substrate and (b) on an insulating substrate; 2D simulated surface current density map at $y=0$ near one electrode for ITO film (c) on conducting substrate and (d) on insulating substrate. (15 mm \times 15 mm \times 2 mm air, 12.7 mm \times 12.7 mm \times 10 μm ITO film, 12.7 mm \times 12.7 mm \times 1 mm substrate, $D = 80 \mu\text{m}$ circular electrodes with a center spacing of 1.5875 mm)

The simulated impedance and capacitance values from 0.1 Hz to 10 MHz for the same 10 μm ITO film also demonstrated that the measurement configurations can cause very big differences in the electrical response (Figure 5). As an example, the impedance magnitude at 1 Hz for an ITO film (12.7 mm \times 12.7 mm \times 10 μm) can change from $5.247 \times 10^{-5} \Omega$ for the parallel-plate configuration to 100.8 Ω for in-plane measurement on an insulating substrate. The real capacitance at 1 Hz can change from $5.712 \times 10^{-10} \text{ F}$ (parallel-plate) to about 10^{-15} F (in-plane). These values can also be used to verify the accuracy of our FEA model. According to the resistance and parallel-plate capacitance Equations 4 and 5:

$$R = \frac{\rho L}{A} = \frac{t}{\sigma a^2} = 5.254 \times 10^{-5} \Omega \quad (4)$$

$$C = \frac{\epsilon_r \epsilon_0 A}{d} = \frac{\epsilon_r \epsilon_0 a^2}{t} = 5.712 \times 10^{-10} \text{ F} \quad (5)$$

where t is the thickness, σ is the conductivity and a is the lateral length of a square ITO film. The theoretical values for resistance and capacitance match the simulation results in the parallel-plate configuration case. This proves that our simulation setup and simulation models are reasonable.

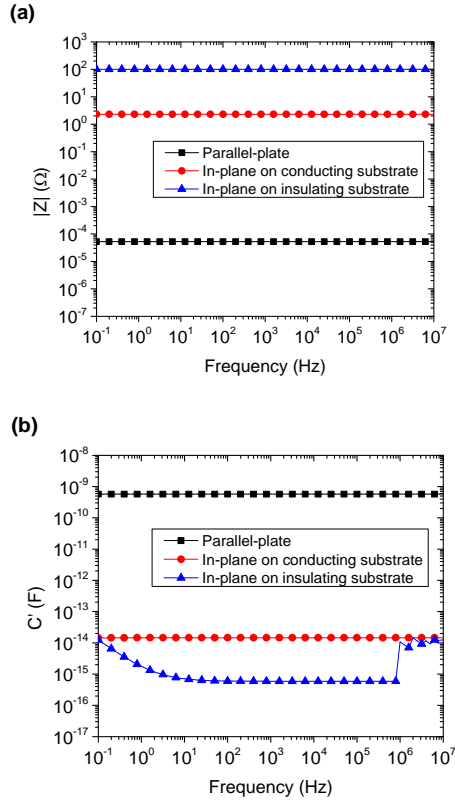


Figure 5. (a) Bode plots of impedance magnitude ($|Z|$) for the same ITO film obtained using three different measurement configurations; (b) Bode plots of real capacitance (C') for the same ITO film with three different measurement configurations.

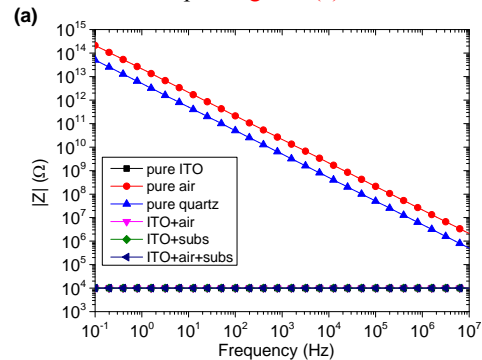
From the simulation results, it is noticed that the parallel-plate configuration and the in-plane configuration with conducting substrate show a relatively low impedance value. Considering the existence of cable and contact resistance, it is very difficult to accurately extract the real ITO film electrical response from real experimental measurements. Also, with very low impedance, the imaginary impedance of the circuit will be dominated by cable inductance which cannot show the correct capacitance behavior. Thus, the in-plane measurement with insulating substrate, which has a relatively large impedance value and minimizes the influence from the environment, is further analyzed in this study. [5]

Effects of substrate and air environment

As insulating materials, the quartz glass substrate and the air environment have large impedance values under normal conditions. Here a 3D model similar to Figure 2(a) was used to simulate the electrical response from a pure ITO film (12.7 mm \times 12.7 mm with thickness of 100 nm), pure quartz glass substrate (12.7 mm \times 12.7 mm with thickness of 1 mm) and air block (15 mm \times 15 mm \times 2 mm). Simplified 3D models using 100 nm ITO film as the electric shielding boundary were applied to simulate the impedance and

capacitance for the combination of ITO film with quartz substrate, combination of ITO film with air, combination of ITO with both substrate and air. In this way, the electrical response for each material can be separated and compared.

Figure 6 shows the simulated impedance and capacitance results for the ITO film, quartz glass substrates, air environment and their combinations. The quartz substrate and air are very insulating and their impedances decrease with increasing frequency. The 100 nm pure ITO film and its three combinations with the surrounding materials have almost the same impedance of $10^4 \Omega$. The imaginary impedances are always insignificantly small (approaching zero) compared to the real impedance. Thus the impedance magnitude is almost equal to the real impedance values. No apparent changes can be observed from 0.1 Hz to 10 MHz, which show a pure resistor behaviour. It was concluded that the substrate and air environment have a very small effect on the impedance of the ITO film as the curves overlap in Figure 6(a).



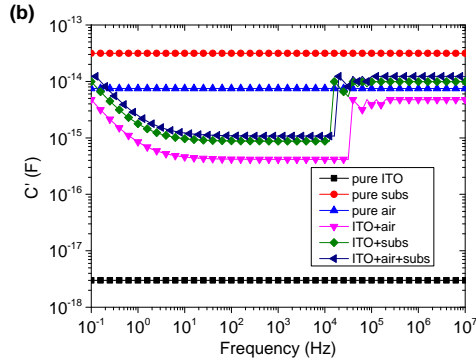


Figure 6. (a) Bode plots of $|Z|$ (b) Bode plots of C' for pure ITO film, pure air block, pure quartz substrate, combination of ITO film with quartz substrate, combination of ITO film with air, combination of ITO with both substrate and air. (15 mm \times 15 mm \times 2 mm air, 12.7 mm \times 12.7 mm \times 100 nm ITO film, 12.7 mm \times 12.7 mm \times 1 mm substrate, $D = 80 \mu\text{m}$ circular electrodes with a center spacing of 1.5875 mm)

However, the capacitance values show very different trends. In the simulation, the pure substrate (3.15×10^{-14} F) and pure air (7.51×10^{-15} F) have much higher capacitance than the pure ITO film (3.00×10^{-18} F, within the estimation of 10^{-19} F to 10^{-17} F) [5]. As a result, the capacitances of combined systems are close to the substrate capacitance and air capacitance, more than 2 orders of magnitude higher than the ITO film capacitance in Figure 6(b) even showing a transition in the middle frequency range (10 to 10^4 Hz). Different air dimensions were simulated, but no apparent differences were observed. It is concluded that the large capacitance of the system proves that in the in-plane capacitance measurement of conducting films on insulating substrates are dominated by the open circuit capacitance (substrate and air). The simulated capacitance for a 100 nm thick ITO film on quartz in air is still 3 orders of magnitude lower than the experimental values ($\sim 1.60 \times 10^{-11}$ F). The main reason may be related to the high capacitance from the probe station and the measuring instrument. With these high capacitances, the real capacitance information of the ITO film are hidden and difficult to be determined from the experiments [5].

Effects of film thickness

Figure 7 shows the impedance and capacitance of ITO films in a wide frequency range simulated by simplified 3D models. The impedance values of ITO films decrease with increasing film thickness in an inverse proportional relationship as shown in Figure 7(a). In addition, the impedance is independent of frequency and shows pure resistive behaviour

because the relaxation frequency is much higher than what is regularly measured.

For pure ITO films, the real capacitance is independent of frequency from 0.1 Hz to 10 MHz (shown in Figure 6(b)). When ITO films are simulated with substrate and air environment, the capacitance curves for different film thickness have similar shapes (displayed in Figure 7(b)). The high frequency plateau and low frequency values for capacitance are always around 1.24×10^{-14} F. The mid-frequency plateau has a capacitance about 10^{-15} F. With increasing film thickness, the sudden drop of capacitance happens at higher frequency. The reason for this transition is still under investigation. It may be due to the large capacitance difference between the conducting film and the environment. When the ITO film is thick enough (100 μm) and has similar capacitance with the environment, the transition disappears (not shown). In the actual measurement, because the open circuit capacitance is so large (10^{-11} F), this phenomenon cannot be measured.

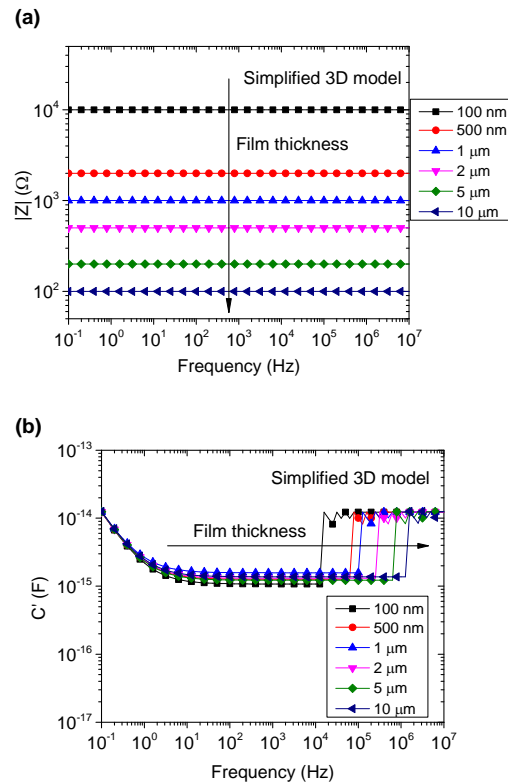


Figure 7. Bode plots of (a) $|Z|$ and (b) C' for ITO films with different thickness on quartz substrate in air environment simulated in simplified 3D models. (15 mm \times 15 mm \times 2 mm air, 12.7 mm \times 12.7 mm \times 1 mm substrate)

Conclusions

Different measurement configurations can cause different measurement results of impedance and capacitance for ITO films. The insulating substrate and surrounding air environment were found to have a substantial effect on the resultant capacitance but minimal influence on the impedance of the films. The impedance values of ITO films decrease with increasing film thickness in an inverse proportional relationship, where the sudden change in capacitance happens at higher frequency with increasing film thickness.

References

[1] Kumar, S., and R. A. Gerhardt. "Role of geometric parameters in electrical measurements of insulating thin films deposited on a conductive substrate." *Measurement Science and Technology* 23, no. 3, 035602. (2012)

- [2] Jin, Y., S. Kumar, and R. A. Gerhardt. "Simulation of the Impedance Response of Thin Films as a Function of Film Conductivity and Thickness." In Proceedings of COMSOL Conference, pp. 1-5. (2015).
- [3] Chen, Y., and J. Juang. "Finite element analysis and equivalent parallel-resistance model for conductive multilayer thin films." Measurement Science and Technology 27, no. 7, 074006. (2016).
- [4] Kumar, S., and R. A. Gerhardt. "Numerical study of the electrical properties of insulating thin films deposited on a conductive substrate." Proc. 2009 COMSOL Multiphysics (Boston, MA, USA) pp. 1-5. (2009).
- [5] Xia, N. "PROCESSING, CHARACTERIZATION AND MODELING OF SOLUTION-PROCESSED INDIUM TIN OXIDE FILMS"; PhD Thesis, Georgia Institute of Technology, Atlanta, GA, (2018).

Acknowledgements

This work was supported by the National Science Foundation under DMR-1207323.